

Torque Teno Virus: Exploring the Effects of Localization on Apoptotic Ability of TTV-VP3

A Major Qualifying Project

submitted to the faculty of

WORCESTER POLYTECHNIC INSTITUTE

in partial fulfillment of the requirements for the

Degree of Bachelor of Science in Biochemistry

by

Celina M. Aherrera

Rashid G. Chatani

Kevin R. Roopcharan

April 30, 2015

Approved by

Dr. Destin Heilman, Advisor

Department of Chemistry and Biochemistry, WPI

This report represents the work of WPI undergraduate students submitted to the faculty as evidence of completion of a degree requirement.

WPI routinely publishes these reports on its website without editorial or peer review.

Table of Contents

ABSTRACT.....	3
INTRODUCTION.....	4
MATERIALS AND METHODS.....	10
RESULTS	16
DISCUSSION.....	21
FIGURES.....	25
REFERENCES.....	30

Abstract

In 2016, cancer is expected to take more than 1,500 lives a day. Human Torque Teno Virus's third viral protein (TTV-VP3) has been shown to induce apoptosis in transformed cells while leaving primary cells unscathed. To design a cancer therapy modelled after TTV-VP3, it is necessary to research its intracellular properties. The steady-state localization of TTV-VP3 has been shown to favor the cytoplasm. It is suspected that amino acids Leu₃₅ and Leu₃₆ are located in the putative NES that interacts with CRM1. Site-directed mutagenesis was performed to mutate these Leucines to Threonines in an attempt to hinder its export capabilities, and drive the steady-state levels of TTV-VP3 to the nucleus. It was determined that Leu₃₅ and Leu₃₆ are not essential for nuclear export but are essential for apoptosis induction.

Introduction

The Torque Teno virus (TTV) was first discovered in 1997 in a Japanese male diagnosed with transfusion-acquired hepatitis. Since the patient tested negative for all known hepatitis viruses, Nishizawa *et al* originally believed that this “Transfusion-Transmitted Virus” was the undiscovered hepatitis-causing pathogen. Though its pathogenicity remains as yet unknown, the virus is thought to be associated with diseases of the liver, respiratory tract, hematopoietic malignancies, and autoimmune diseases (1). However, epidemiological studies showed that TTV is present in over 90% of the adult human population, meaning that it is present in both healthy and diseased individuals. The ubiquity of TTV in human adults suggests a strong connection to its human host, though no evidence has ever been found that might indicate TTV’s relationship to humans (2).

The virus has a single-stranded, circular, antisense DNA genome of length 3.8 kb (2). Nishizawa *et al* first began characterization of TTV by isolating a viral clone (N22) of 500 nucleotides from the serum of the infected patient. The N22 clone was found to contain an ORF that was capable of encoding at least 166 amino acids. The National Institute of Genetics in Japan was unable to find a single known sequence to have high homology to the N22 clone. Additionally, no protein sequences indicated a high homology to the amino acid sequence of the viral clone’s ORF. Further investigations discovered that TTV shared some characteristics with the *Circoviridae* family. Like TTV, circoviruses are non-enveloped and contain circular, single-stranded DNA with either positive or ambisense polarity. Though the particle size and genome size of TTV are larger than those of known circoviruses (1.7-2.3 kb DNA), they possess similar densities in CsCl, which indicates similarities in their protein-to-DNA ratios (3).

As a member of the *Circoviridae* family, TTV shares similar characteristics with other circoviruses falling under this category, including the chicken anemia virus (CAV), which causes transient anemia, bone marrow atrophy, and severe immunosuppression in chickens. CAV has a 2.3 kb single-stranded circular DNA. Its genome codes for three viral proteins (VP1, VP2, and VP3) in three overlapping open reading frames, all of which are necessary for the virus to replicate (4). CAV-VP3, also known as Apoptin, has been widely studied because of its novel ability to selectively induce apoptosis in human cancer cells. The protein is composed of 121 amino acids; amino acids 97-105 contain a putative nuclear export sequence (NES), and amino acids 82-88 and 111-121 each contain nuclear localization sequences (NLS) (4). These recognition sequences are responsible for the observed nucleocytoplasmic shuttling behavior of Apoptin (5). This shuttling behavior is believed to play a role in Apoptin's apoptotic ability as well.

Research shows that Apoptin localizes mainly in the nucleus of cancer cells and in the cytoplasm of normal cells, which suggests that its nuclear localization is necessary for inducing apoptosis (6). Heilman *et al.* showed that in transformed cells, Apoptin associates with subunit 1 of the anaphase-promoting complex/cyclosome (APC/C). The APC/C is a complex protein that is responsible for activating separase, a cysteine protease that triggers anaphase during the cell cycle. Apoptin has been shown to inhibit APC/C upon binding to subunit 1, leading to G2/M cell cycle arrest. The inhibition of an important cell cycle regulator eventually leads to mitochondrial apoptosis through the Nur77 pathway, a p53-independent pathway (4, 5).

The p53 protein is a widely studied tumor suppressor and plays an important role in how the body defends itself against cancer. The p53 protein is coded for by the TP53 gene. When p53 binds DNA, it stimulates the production of the p21 protein, which interacts with CDK2, a cell

division-stimulating protein. With the presence of this CDK2/p21 complex, the cell is effectively arrested in the cell cycle (7). In addition to causing cell cycle arrest, the p53 protein is also capable of activating DNA repair mechanisms and apoptosis. The p53 pathway is the primary pathway that a cancer cell will take in initiating apoptosis. However, in nearly half of naturally occurring cancers, the p53 pathway is mutated, emphasizing the importance of a p53-independent apoptotic pathway (6). Both Apoptin and TTV-VP3 operate via a p53-independent pathway, emphasizing their potential as cancer therapies.

The Torque Teno Virus, like Apoptin, contains three conserved spliced mRNAs. These mRNAs are of lengths 3.0, 1.2, and 1.0 kb, and are known as ORF1, ORF2, and ORF3, respectively (8). Of particular importance to this research is ORF3, which is known to code for the TTV-VP3 protein, a homologue of Apoptin (9). Like Apoptin, TTV-VP3 is able to selectively kill cancer cells while leaving primary cells intact. The mechanism by which this protein induces apoptosis is even less clear, however. Previous studies were able to provide evidence for the existence of an NES as well as an NLS on TTV-VP3 (10). The first 78 amino acids of the 105 amino acid chain contain the nuclear export sequence (NES), and the remaining portion contains the nuclear localization sequence (NLS) (10). A study conducted in 2011 truncated TTV-VP3 into these two pieces, and found that the NES truncation localized in the cytoplasm 69% percent of the time, while the NLS truncation localized in the nucleus 64% of the time, indicating that these two fragments were indeed functional (10). Although the NLS and NES of TTV-VP3 are functional, the protein does not display the same nucleocytoplasmic shuttling behavior that Apoptin does. Rather, TTV-VP3 maintains a steady-state localization with higher levels of the protein in the cytoplasm of both cancerous and normal cells (11).

The nucleocytoplasmic shuttling behavior of Apoptin is carried out by the intracellular mechanisms that continually transport the protein across the nuclear membrane. Although TTV-VP3 does not display this shuttling, its steady-state localization in the cytoplasm may also be maintained by these transport mechanisms. Since only small molecules (20-40 kD) can passively diffuse across the nuclear membrane, large molecules require signal-dependent and energy-dependent mechanisms in order to accomplish transport across the nuclear membrane. CRM1 (Chromosomal Maintenance 1) is the major export protein in mammalian cells responsible for facilitating transport of a variety of macromolecules from the nucleus to the cytoplasm (12). Upon making contact with CRM1's hydrophobic binding pocket, the macromolecule to be transported undergoes a conformational change to bind to CRM1. The majority of the export substrates of CRM1 contain a leucine-rich region in the NES of the substrate, indicating that these conserved leucines may be essential for the protein to be recognized by CRM1 (13). Binding of CRM1 to the molecule of interest also occurs cooperatively with RanGTP. The Ran protein is a small GTPase that is essential in determining the directionality of the nuclear transport; it shuttles between compartments through the nuclear membrane in order to complex with incoming and outgoing macromolecules. The resulting CRM1/cargo protein/RanGTP complex then docks at the nuclear pore complex (NPC), the site of active transport between the nucleus and the cytoplasm, where it is transported to the other side of the nuclear envelope (12). On the cytosolic side of the nuclear envelope, GTP hydrolysis and the release of RanGDP lead to the dissociation of the complex; the bound cargo protein is then released from CRM1 and into the cytoplasm.

The importance of the localization of TTV-VP3 remains undetermined, but the structural similarity of the protein to Apoptin suggests that it might induce cellular apoptosis in a similar

manner. Because its apoptotic induction is selective for cancer cells, TTV has the potential to be utilized in cancer therapies. It is important to note that if induction of apoptosis relies on a change in localization, developing a therapy in the form of administered drugs becomes exceedingly difficult. A naturally occurring protein is complex enough to support a conformationally regulated change in localization behavior, whereby it is moved into another cellular compartment. A small molecule, which lacks a complex structure, will be unable to achieve the conformational change necessary to drive it into another cellular compartment. On the other hand, the killing mechanism may not involve a specific localization of the protein. If that is the case, then it may be easier to develop a drug that mimics these proteins' mechanism of action since the subcellular localization is nonessential to the killing mechanism.

Project Overview

This investigation will focus on characterizing the killing capacity of Torque Teno Virus—specifically, the NES-containing region of the protein—in relation to its subcellular localization. Since leucine-rich residues are highly conserved in many known nuclear export sequences,^[CA7] it seemed logical to create point mutations on the NES in order to alter the protein's localization. These mutations are intended to push the steady-state localization of TTV-VP3 toward the nucleus. Leucine 35 and Leucine 36 were selected for site directed mutagenesis based on the results of NetNES (14). NetNES is comprised of two prediction softwares that assigns an NES Score to each amino acid in a specified sequence. The NES Score is a quantified measure of the probability of each amino acid's involvement in the nuclear export motif. The results that were used to corroborate the selection of the site directed mutagenesis are shown below in Figure 1. The localization of the TTV-VP3 $\Delta\Delta$ LL35-36TT mutant will be compared to that of the wild-type under epifluorescence and laser confocal microscopy. Then, an apoptosis

assay will be used to quantify the killing capabilities of both the mutant and wild-type proteins (15). If TTV-VP3 $\Delta\Delta$ LL35-36TT possesses a different localization pattern than wild-type TTV-VP3, and still demonstrates the ability to induce apoptosis, then it can be concluded that the protein's localization is not involved in its apoptotic mechanism. If a change in localization significantly hinders the protein's ability to kill, then it can be concluded that the killing mechanism does rely on the subcellular localization of TTV-VP3.

Materials and Methods

Site-Directed Mutagenesis via QuikChange Cloning

Two primers (one forward and one reverse) were designed to mutate two leucine residues to threonine residues on the putative NES of TTV-VP3. The targeted wild-type sequence was 5'CGCTCATTTTAATCATCTTGGAAGACTGCTTCGTGCCCCGCAAAAC'3, with the underlined residues indicating the two leucine residues that were intended for mutation.

The forward primer sequence was 5'CGCTCATTTTAATCATCTTGACTACTTGCTTCGTGCCCCGCAAAC'3 and the reverse primer sequence was 5'GTTTTGCGGGGCACGAAGCACTTCTGCAAGATGATTAAAATGAGCG'3. The underlined portions of the primers are the two new threonine residues that were incorporated during Quikchange PCR. These primers were used to carry out a QuikChange PCR with the following contents: 10X reaction buffer (5 μ L), DNTP mix (1 μ L), PFU polymerase (1 μ L), Forward Primer (2.5 μ L), Reverse Primer (2.5 μ L), TTV Wt DNA template (1 μ L), and Nuclease free water (35.5 μ L). A negative control was prepared by replicating the above conditions without the primers and maintaining the same total volume by increasing the volume of nuclease-free water. The PCR program was run as follows: 1 cycle at 95°C for 4 minutes, 30 cycles of 95°C for 30 seconds, 65°C for 1 minute and 72°C for 4 minutes, and 1 cycle at 72°C for 5 minutes. The product was then cooled to a temperature of 10°C for holding, and then stored at -20°C. In order to digest template DNA, *DpnI* (2 μ L) was added to each PCR reaction. The tubes were incubated at 37°C for at least 1 hour. Prior to digestion, 5 μ L of experimental product was transferred to Eppendorf tubes for use as positive controls.

Transformation of Competent JM109 E. coli

PCR product (2 μL) was added to tubes of competent JM109 *E. coli* (50 μL) and incubated on ice for 20 minutes. Tubes were then heat shocked at 42°C for 1 minute, and then immediately placed back on ice for another 2 minutes. Pre-warmed LB broth (450 μL) was added to each tube following incubation. The tubes were placed in a shaking incubator and allowed to recover for 1 hour at 37°C. The 150 μL of the cells were plated on LB agar plates containing kanamycin, and incubated for 24 hours at 37°C.

Plasmid Miniprep

Colonies from successful transformations were inoculated in falcon tubes with LB-broth (3 mL) containing kanamycin (3 μL). These were incubated in the shaking incubator overnight at 37°C. The following day, the plasmid DNA was purified using the Promega PureYield Plasmid Miniprep System. In an Eppendorf tube, bacteria culture (1 mL) was centrifuged at 10,000 rpm for 30 seconds. The supernatant was decanted, and the process was repeated so that a total of 2 mL of bacteria culture were pelleted. Cell pellets were resuspended in cell resuspension solution (600 μL). Cell lysis buffer (100 μL) was added. Cells were allowed to lyse for 1 minute by inverting the tube and gently vortexing. Lysis was stopped by adding neutralization solution (350 μL) and gently vortexing until the blue color of the lysis buffer had disappeared. The lysate was centrifuged at 10,000 rpm for 30 seconds. The supernatant (900 μL) was transferred into a minicolumn and centrifuged at 10,000 rpm for 30 seconds. After discarding the flow-through, endotoxin removal wash (200 μL) was added and the column was centrifuged again at 10,000 rpm for 30 seconds. Column wash (400 μL) was added and the column was centrifuged at 10,000 rpm for 30 seconds. The flow-through was discarded again, and an additional centrifugation was run at 10,000 rpm for 1 minute to elute any residual solutions. The minicolumns were transferred to autoclaved Eppendorf tubes and elution buffer (30 μL) was added to the tube. The tubes were

centrifuged at 10,000 rpm for 30 seconds, then stored at -20°C. A UV spectrophotometer was used to determine the concentration of the purified DNA. The DNA was then sent out to Macrogen USA for sequencing, and the sequences were analyzed for the presence of the mutation.

Midiprep Plasmid Purification

PCR product (2 µL) was added to a tube of JM109 *E. coli* (50 µL) and incubated on ice for 20 minutes. The tube was then heat shocked at 42°C for 1 minute, and then immediately placed back on ice for another 2 minutes. The cells were then added to 50 mL of LB broth with 50 µL of Kanamycin. The culture was grown overnight at 37°C. The next day plasmid DNA was purified using the Promega PureYield Plasmid Midiprep System. The culture (50 mL) was transferred into a centrifuge tube and centrifuged for 10 minutes at 5,000 g. The supernatant was removed and the pellet was resuspended in cell suspension solution (3 mL). Cell lysis buffer (6 mL) was added and the tube was vortexed for 3 minutes to ensure complete lysis. Neutralization solution (10 mL) was added to stop lysis. The tube was vortexed again for 2 minutes. The mixture was centrifuged at 15,000 g for 15 minutes. The supernatant was poured into a wash column attached to a binding column. The columns were attached to a vacuum manifold powered by a vacuum pump. Once the vacuum was applied, and the supernatant run through, the clearing column was discarded. Endotoxin removal wash (5 mL) was added to the tube and allowed to flow through. Column wash solution (20 mL) was added to the column and allowed to flow through. The column was placed in a 50 mL conical tube and pre-warmed (55°C) ddH₂O (600 µL) was applied to the column. The tube was centrifuged for 5 minutes at 3,000 g. The flow-through was transferred to a clean Eppendorf tube. The concentration was analyzed using a UV Spectrophotometer. The purified DNA was stored at -20°C.

Transfection of H1299 Cells

H1299 non-small lung carcinoma cells were passed into a 6-well plate containing glass coverslips at approximately 50% confluence the day before transfection. On the day of transfection, 0.8 µg of DNA was diluted to a final volume of 200 µL using EC buffer. Enhancer was added (6.4 µL) and the tube was vortexed and allowed to incubate at room temperature for 5 minutes. Effectene reagent (20 µL) was added drop-wise and the mixture was incubated for 10 minutes at room temperature to allow for complex formation. During the incubation period, growth medium was aspirated from the cells on the 6-well plate. The cells were washed once with PBS and 1.5 mL of fresh media was added to each well. After the 10-minute incubation, fresh media (1.2 mL) was added to the complexes and pipetted up and down to mix. The mixture (400 µL) was added drop-wise to each of two wells. The plate was then returned to the 37°C incubator overnight. The volumes of DNA in EC buffer, Enhancer, and Effectene reagent were each added to two wells in the 6-well plate.

Preparation for Fluorescence Microscopy

The cell culture media was aspirated out of the 6-well plates. The wells were washed with PBS, which was then aspirated off. Paraformaldehyde (4% in PBS, 1 mL) was applied to each well and gently rocked on a nutator for 15 minutes. The paraformaldehyde was aspirated off and the cells were washed with PBS (1 mL). EtOH (70% in 2 mL) was added to each well to preserve the cells. The plates were covered using parafilm and stored at 4°C. The coverslips were removed from the wells and mounted on glass slides. Before applying the coverslips to the slides, mounting media with DAPI (10 µL) was applied. The slides were pressed gently with a paper towel to remove excess mounting media. The edges of the slides were sealed with clear nail polish. Cells were viewed under laser fluorescence microscopy to determine localization of the proteins.

Cell Viability Assay

Cells were cultured in 6-well dishes. Transfections were carried out when the cells were at 60-80% confluence. Two wells were left unaltered for use as controls. One well was used for transfection-negative, G418-positive treatment and the other well was used for transfection-negative, G418-negative treatment. After 24 hours, the cells were examined under a fluorescent microscope to confirm that the transfections were successful and that the transfection efficiencies were similar. Transfection efficiencies were between 30-40%. When confluence exceeded 90%, the first geneticin selection was carried out. Culture media was aspirated off and the wells were washed with ~2 mL of 1% PBS. The PBS was aspirated off and 0.2 mL of 0.05% trypsin was added to each well. The trypsin was aspirated off after ~20 seconds. The cells were resuspended in 2 mL of media mixed with 800 µg/mL G418 using a P1000 micropipette. The cell suspension (0.825 mL) was transferred to a new 6-well dish and 1.275 mL of G418 media was added to work up the volume to 2 mL. The G418-negative well was treated the same way except G418-negative media was used. Two days later, the media was aspirated off and the wells were washed with ~1.5 mL 1X PBS. G418 media (2 mL, 1200 µg/mL) was added to each well. G418-negative media was added to the "No trans -" well. Two days later, the same process was repeated except 2 mL of 800 µg/ml were added to the appropriate wells. After two days, crystal violet staining was used to visualize all remaining viable cells. All solutions were pipetted onto the wall of the wells and allowed to disperse gently while rotating the plate. This was done to avoid detaching the cells. The media was aspirated off and the cells were washed with ~1 mL of 1% PBS. The PBS was aspirated off and the cells were fixed using 4% paraformaldehyde prepared in 1% PBS. The cells were allowed to be fixed with -20°C ethanol by nutating for 15 minutes. Crystal violet prepared in 10% ethanol (0.75 mL, 0.1% (w/v)) was added, and the cells were allowed to be stained over 20 minutes. The wells were washed with distilled water until the water ran clear.

This was done to remove the excess staining agent. Pictures were taken of the wells for visual evaluation and the wells were dried overnight. The staining agent was solubilized by 2% (w/v) sodium dodecyl sulfate (SDS). Using a Genesys 20 Visible Spectrophotometer (Thermo Scientific), the wells' optical densities were measured at 590 nm. The dyes were diluted if the concentration of the dye was too high for the spectrophotometer to detect. Cell Viability was calculated: $OD \text{ of experimental} / OD \text{ of control} \times 100\% = \text{Cell viability}$.

Results

Torque Teno Virus viral protein three (TTV-VP3) has been shown to selectively kill cancer cells without the presence of a functional p53 protein. This capacity to induce apoptosis makes TTV-VP3 a protein of interest in cancer treatment research. Understanding the intracellular properties of this protein is the first major step in the development of a treatment. One characteristic of TTV-VP3 that has been hypothesized to play a role in its killing ability is its higher levels of steady-state localization in the cytoplasm. This steady-state localization is maintained through the protein's NES--located between amino acids 1-78--and NLS, located on amino acids 79-105. Since the NES is believed to be critical for both cytoplasmic localization and killing capacity, this project centered around knocking out the NES to shift the steady-state levels of TTV-VP3 from the cytoplasm to the nucleus, and then observing if the altered localization affected killing capacity. Based on the NetNES prediction software, Leucine 35 and Leucine 36 have a high probability of being linked to the nuclear export mechanism of TTV-VP3 (Fig. 1). In order to assess the importance of these residues in the export mechanism of TTV-VP3, the hydrophobic leucine residues were mutated to hydrophilic threonine residues with the aim of interfering with the NES's binding capabilities to CRM1. The mutant construct was created by mutating Leucine 35 and Leucine 36 in the wild-type protein (5'CTTCTG'3) to threonine residues (5'ACTACT'3). This mutant construct, named TTV-VP3 $\Delta\Delta$ LL35-36TT, was generated via Quikchange PCR, which utilized thermal cycling to introduce the desired threonine mutations into the parental plasmid (Fig. 2). Using the TTV wild-type plasmid as a template, the initial heat cycle denatured the DNA to separate the strands. The second cycle allowed primers—designed to include the threonine residues at amino acid positions 35 and 36—to anneal to the targeted site on the parental plasmid. The third cycle elongated the annealed primers,

incorporated the threonine residues, and resulted in a new plasmid. Several rounds of thermal cycling resulted in many copies of the new TTV-VP3 $\Delta\Delta$ LL35-36TT plasmid. The parental plasmids not containing the mutation were digested using *DpnI*, and the plasmids expressing TTV-VP3 $\Delta\Delta$ LL35-36TT were transformed into *E. coli*. After plating the bacteria on selective media, picking colonies, and purifying the DNA, the sample was sent out for sequencing to confirm that it contained the mutation of interest. The successful incorporation of the desired point mutations into the construct is shown in the electropherograms (Fig. 3).

In order to assess whether the point mutations affected the protein's steady-state localization, plasmids expressing constructs TTV-VP3 $\Delta\Delta$ LL35-36TT were transfected into H1299 non-small lung carcinoma cells. The cells were grown on glass coverslips in a 6-well plate at a confluence of ~70% on the day of transfection. Plasmids expressing only GFP were also transfected to establish a control for the localization of GFP in the transformed cell, and plasmids expressing Wild-Type TTV-VP3 were transfected as well. After twenty-four hours, the cells were fixed on glass slides and the localization of each protein in the cell was observed under laser confocal microscopy. The localization of TTV-VP3 $\Delta\Delta$ LL35-36TT was compared against the localization of TTV-VP3 wild-type to assess the importance of Leu₃₅ and Leu₃₆ in nuclear export. Two additional constructs—plasmids expressing truncations of TTV-VP3 (amino acids 1-78 called NES, and amino acids 79-105 called NLS)—were procured from a previous research project and sequenced to confirm the identity of the constructs (10). These were also transfected into cells to confirm that the NES alone was able to localize the protein to the cytoplasm, and that the NLS alone was able to localize the protein to the nucleus.

Successfully transfected cells exhibit fluorescence under the confocal microscope when viewed with a GFP filter. The cell transfected with GFP shows the protein to be diffuse

throughout the entire cell. The truncated NES displays fluorescence mostly in the cytoplasm of the cell, confirming that the NES is functional on its own. The truncated NLS demonstrates its ability to be shuttled into the nucleus, which also confirms that the NLS is functional. The wild-type TTV-VP3 protein visually displays higher levels of fluorescence in the cytoplasm than in the nucleus of the cell, as expected. The TTV-VP3 $\Delta\Delta\text{LL35-36TT}$ protein displays similar levels of cytoplasmic fluorescence to the wild-type TTV-VP3. Figures 4A and 5A show the subcellular localization of each of the constructs described above. Although it is possible to make conclusions on each protein's subcellular localization qualitatively, it was necessary to quantify the cells' fluorescence to validate the localization of each construct. In order to quantify the localization of each construct, a representative cell transfected with the construct of interest was chosen and GFP fluorescence was measured using ImageJ. Fluorescence intensities were calculated for the nucleus and cytoplasm of the construct, and then used to calculate the corrected total cell fluorescence (CTCF). These values were found by subtracting the product of the selected area of the cell and the mean fluorescence background reading from the integrated density of the selected cell. The nuclear-to-cytoplasmic ratio of GFP expression of the cell was then calculated. The values were normalized against the calculated values for TTV-VP3 $\Delta\Delta\text{LL35-36TT}$. The data shows that the NLS truncation was more localized in the nucleus with a ratio of 0.707, compared to 0.150 for the NES truncation, which was mostly localized in the cytoplasm (Fig. 5B). These ratios confirm that the NES is capable of being localized to the cytoplasm, and that the NLS can move to the nucleus. Additionally, the wild-type construct showed a nuclear-to-cytoplasmic ratio of 0.242, and the TTV-VP3 $\Delta\Delta\text{LL35-36TT}$ construct had a ratio of 0.210 (Fig. 4B). These ratios indicate that both TTV-VP3 wild-type and TTV-VP3 $\Delta\Delta\text{LL35-36TT}$ remained localized largely in the cytoplasm, which corresponds to the

fluorescence observed in the confocal images. The results of a two-tailed T test between the N/C ratios of TTV-VP3 wild-type and TTV-VP3 $\Delta\Delta$ LL35-36TT gave a *P* value of 0.982. Since this value is greater than 0.05, the data has no statistical significance [*P*-value=0.982, *P*>0.05]. This data suggests that neither Leu₃₅ nor Leu₃₆ are involved in the nuclear export mechanisms of TTV-VP3.

Though the TTV-VP3 $\Delta\Delta$ LL35-36TT construct did not change its localization to favor the nucleus, it was still unknown whether the mutant construct retained its ability to kill transformed cells. In order to determine if the mutant construct could still kill, the mutant-expressing plasmid was transfected into H1299 cells and a viability assay was performed, which took advantage of the neomycin resistance built into the plasmids containing the constructs (15). For the assay, H1299 cells were grown in a 6-well plate and transfected with the constructs of interest. Twenty-four hours after transfection, transfection efficiencies were measured under fluorescence microscopy since transfection efficiencies needed to be similar for the assay to produce valid results. Transfection efficiencies were between 20% - 40% for each well. At this point, the wells were treated with G418-laced media. G418, a homolog of neomycin, kills only transfection-negative cells since transfection-positive cells express the resistance gene. The cells were put under G418 selection for six days, where after two days the concentration of G418 was increased to ensure that only transfection-positive cells survived. After four days the cells were allowed to recover, as too much of the drug can overwhelm the cells if they are not producing the resistance gene fast enough. Then, the cells were fixed using cold ethanol and the viable cells were stained with crystal violet in order to be able to visualize them under microscopy. The cell viability was quantified by measuring the relative absorbance of crystal violet present in each well. There were three controls: a transfection-negative well treated with G418, a transfection-

negative well without G418, and a well transfected with an empty GFP vector. The drug-treated transfection-negative control well had essentially no viable cells, as expected. The transfection-negative control well treated with drug-free media produced a lawn. This validated that G418-laced media kills all transfection-negative cells. All transfection-positive cells are resistant to G418. The constructs that were put through the viability assay were the Wild-Type TTV-VP3, TTV-VP3 $\Delta\Delta\text{LL35-36TT}$, and NLS (Fig. 6A, 6B).

While conducting the viability assay, it became quite evident by the sixth day that cells transfected with $\Delta\Delta\text{LL35-36TT}$ and NLS were still mitotically active. They were more confluent than the empty GFP vector control with many neighbors that could be daughter cells of a mitotic division. At that point, they had been under G418 selection for five days. The only way the cells could be alive and mitotic is if they were expressing G418 resistance. Being mitotically active means that they were not being killed by the expressed construct either. Through these observations, we concluded that the $\Delta\Delta\text{LL35-36TT}$ and NLS constructs are not lethal to cancer cells. On the contrary, cells transfected with Wild-Type TTV-VP3 showed little to no mitotic activity. Under 100x magnification, cells were dispersed sparsely throughout the plate. These cells had no nearby neighbors, indicating that they had not undergone mitosis since being transferred to the well. This observation, combined with the confluence relative to the empty GFP vector control confirmed that TTV-VP3 Wild-Type construct is lethal to cancer cells.

Discussion

The human Torque Teno Virus VP3 protein exhibits high homology to the Chicken Anemia Virus protein Apoptin in both structure and function. Like Apoptin, TTV-VP3 has the ability to induce apoptosis in cancer cells while leaving primary cells unharmed, making the study of the protein an interesting subject for cancer research. Though the TTV-VP3 protein may exist in both subcellular compartments, it demonstrates an equilibrium with a higher steady-state localization in the cytoplasm of both cancer and primary cells. This is contrary to Apoptin, in that Apoptin kills when localized in the nucleus of cancer cells. Since the subcellular localization of Apoptin is believed to be linked to the protein's ability to kill, it is important that the relationship between the steady-state localization of TTV-VP3 and its killing capacity be researched as well.

The laser confocal microscopy images of the NES and NLS truncation corroborate data from previous research that the sequences are functional and produce the reported steady-state localization. The NES fragment exhibits a stronger influence over the localization of the protein than the NLS fragment, as the Wild-Type TTV-VP3 localizes in the cytoplasm. Analysis of the protein sequence through the NetNES prediction software revealed an eight-residue nuclear export motif spanning residues 29-39. The residue consists of seven leucines and one valine. The software predicted that Leu₃₅ and Leu₃₆ are part of the nuclear export motif.

The only differences between Wild-Type TTV-VP3 and TTV-VP3 $\Delta\Delta$ LL35-36TT are the mutations of Leu₃₅ and Leu₃₆ to threonine residues. The initial intention of mutating these residues was to diminish the protein's nuclear export capabilities, The microscopy images of the Wild-Type TTV-VP3 and the TTV-VP3 $\Delta\Delta$ LL35-36TT protein show that the mutation did not significantly alter the steady-state localization of TTV-VP3 $\Delta\Delta$ LL35-36TT, as it remains largely

in the cytoplasm. Even though these residues were predicted to be involved in the nuclear export motif of the Wild-Type protein, there was no statistical difference between the nuclear-to-cytoplasmic ratios of CTCF for each construct. This result suggests that Leu₃₅ and Leu₃₆ are nonessential to the nuclear export mechanism, which is contrary to the NetNES's prediction. Another reason could be that mutation did not induce a conformational change that was significant enough to modify the structure of the NES in such a way that would disturb its interaction with CRM1, and thus, modify the steady-state localization. It is also possible that the methyl groups on the threonine residues are still able to interact with the hydrophobic binding pocket on CRM1. If that were the case, then another residue such as serine may be better suited to knocking out the NES, since its -OH group sticks straight out from the molecule with no other large hydrophobic groups interfering. The data may also imply that CRM1 is not the export protein utilized by the TTV-VP3 NES, and that a different protein is responsible for bringing TTV-VP3 to the nuclear pore complex. Although leucine-rich residues have been shown in the literature to be involved in export mechanisms, Leu₃₅ and Leu₃₆ are likely not involved in this particular NES's export capabilities. However since the NES prediction software had predicted the involvement of only a few residues in the NES, we can speculate that there is still the possibility that another residue within the sequence is responsible for the export mechanism. Perhaps another leucine residue could be a point of interest in altering the protein's localization.

Although steady-state localization was not altered, the ability to induce apoptosis was lost or significantly reduced. These findings indicate that Leu₃₅ and Leu₃₆ are necessary for catalytic activity of Wild-Type TTV-VP3. Mutating these residues may have induced a conformational change of the secondary or tertiary protein structure in a binding site necessary for the mechanism of apoptosis. Alternatively, Leu₃₅ and Leu₃₆ may be catalytically active in inducing

apoptosis, in which case they would reside in a binding pocket of the protein. Mutating residues in the binding pocket would likely destroy the catalytic activity of the binding site. A third possible explanation for the loss of function is that the mutated residues caused a conformational change in the enzyme that resulted in GFP sterically blocking the binding site. Filativa and Vu provided evidence that GFP could be sterically inhibiting substrate-binding in their GFP-Apoptin fusion (15). In this case, the steric hindrance resulting from the conformational change would be responsible for the loss of function and not the residue mutations. The initial goal of this project was to knock out the NES function by mutating Leu₃₅ and Leu₃₆, which were thought to be essential for nuclear export. However, it seems that the data contradicts this hypothesis and shows us that the leucines may reside not on the region for export, but the region for killing. Thus, it was surprising to find that the residues were nonessential for nuclear export but essential to apoptosis induction.

The NLS construct proved to be nonlethal to cancer cells. This result does not necessarily mean that amino acids 79-105 are not essential for apoptosis induction via Wild-Type TTV-VP3. The polypeptide stretch may contain portions of the binding pockets or allosteric sites that are useless without the rest of the construct. The NLS may have apoptotic ability on its own. While unlikely, the fusion of the NLS to GFP could result in steric inhibition of function as speculated with the GFP-Apoptin construct. No substantial conclusions can be drawn from the viability assay showing that NLS is non-lethal.

Future Investigations

Since this project only studied the effects of one leucine-to-threonine mutant construct, it would be prudent to create a different mutant construct in order to try to alter the localization of TTV-VP3. Future research could investigate the effect of mutating the same leucine residues to

alanine residues. This mutation would primarily assess how a change in residue length--rather than hydrophobicity--would have on the NES. Another construct could be generated that mutates the leucine residues to serine residues, since the -OH group is more accessible to the hydrophobic binding pocket of CRM1 and may better inhibit binding. Since the NES Server prediction software has shown that there is only one possible putative export sequence, another option would be to introduce point mutations at different residues on the NES (such as Leu₂₉, Leu₃₁, Leu₃₂, Leu₃₃, Leu₃₅, Leu₃₆, or Leu₃₉) to assess the effect of the mutations at different locations. These changes may be more successful in significantly altering the steady-state localization of TTV-VP3, which would allow future researchers to obtain more conclusive data on the relationship between the protein's killing capacity and its localization. Most importantly, understanding this relationship could be the next step to providing future generations with successful cancer therapies.

Figures

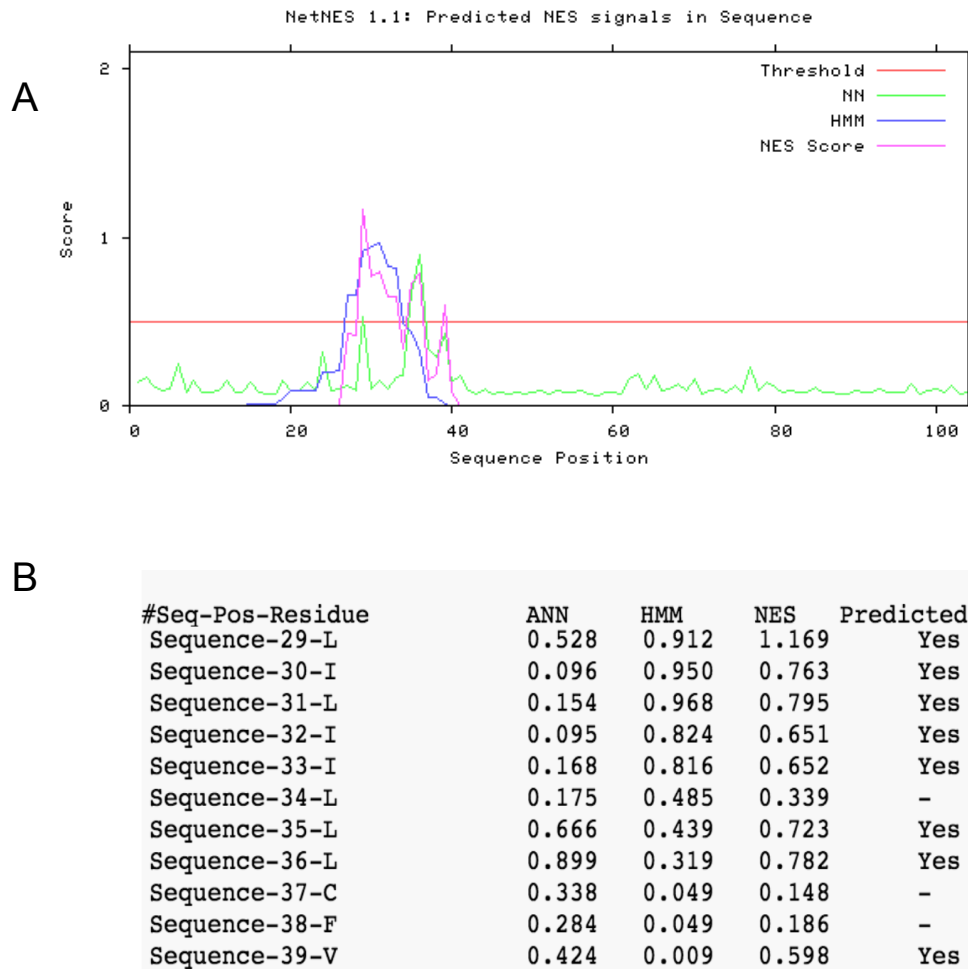


Fig. 1A. Predictive model of polypeptide nuclear export capabilities. Each integer of the horizontal axis represents amino acids of Wild-Type TTV-VP3 starting from the N-terminus to the C-terminus. The vertical axis scores these amino acids on their likelihood to interact with the CRM1 protein and induce nuclear export. The green and blue lines represent two different predictive models designed by Anders Krogh at the University of Denmark in 1998. The pink line indicates the overall score for each amino acid. The red line shows the threshold score needed to be considered as part of a nuclear export motif. Amino acids 29-39 are predicted to be involved in nuclear export. **Fig. 1B.** A table showing the prediction scores for amino acids 29-39 of Wild-Type TTV-Vp3. Amino acids 29-33, 34-35, and 39 score above 0.5 for the NES prediction and are therefore predicted to be involved in the nuclear export motif.

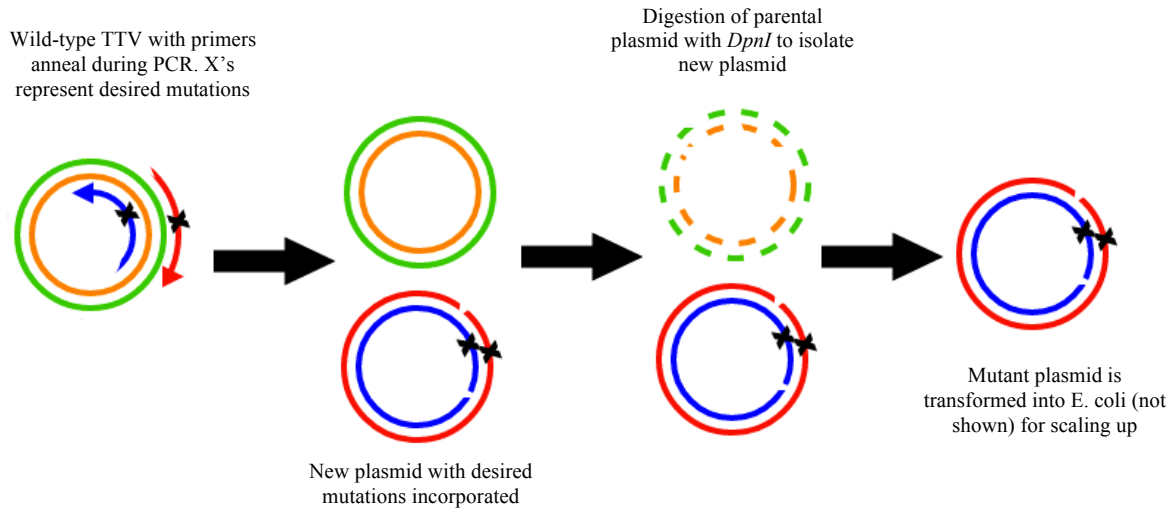


Fig. 2. Introduction of point mutations via Quickchange PCR. Primers with desired mutations (red and blue arrows) anneal to the parental plasmid (green and orange circles) and incorporate mutations (black X's) into a new plasmid containing staggered nicks (red and blue circles). The X's represent the desired threonine residues that will be part of the TTV-VP3 $\Delta\Delta LL35-36TT$ mutant protein. Next, *DpnI* digests the parental plasmid in order to isolate the new mutated plasmid. The new plasmid is transformed into JM109 *E. coli* where the nicks are repaired by DNA ligase.

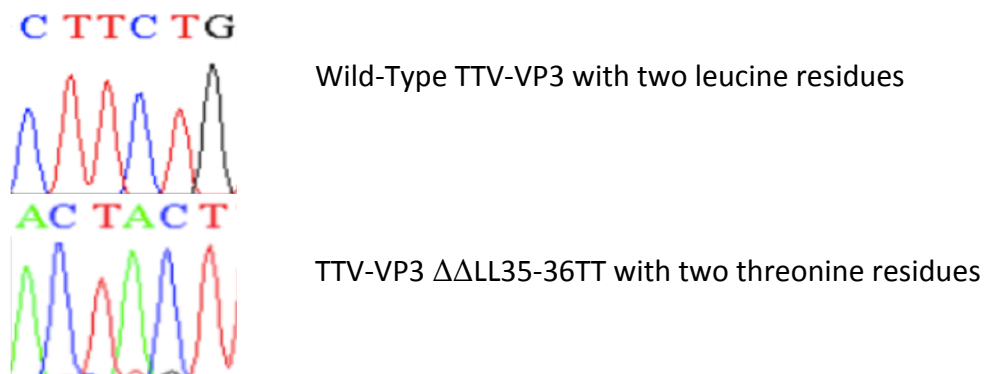
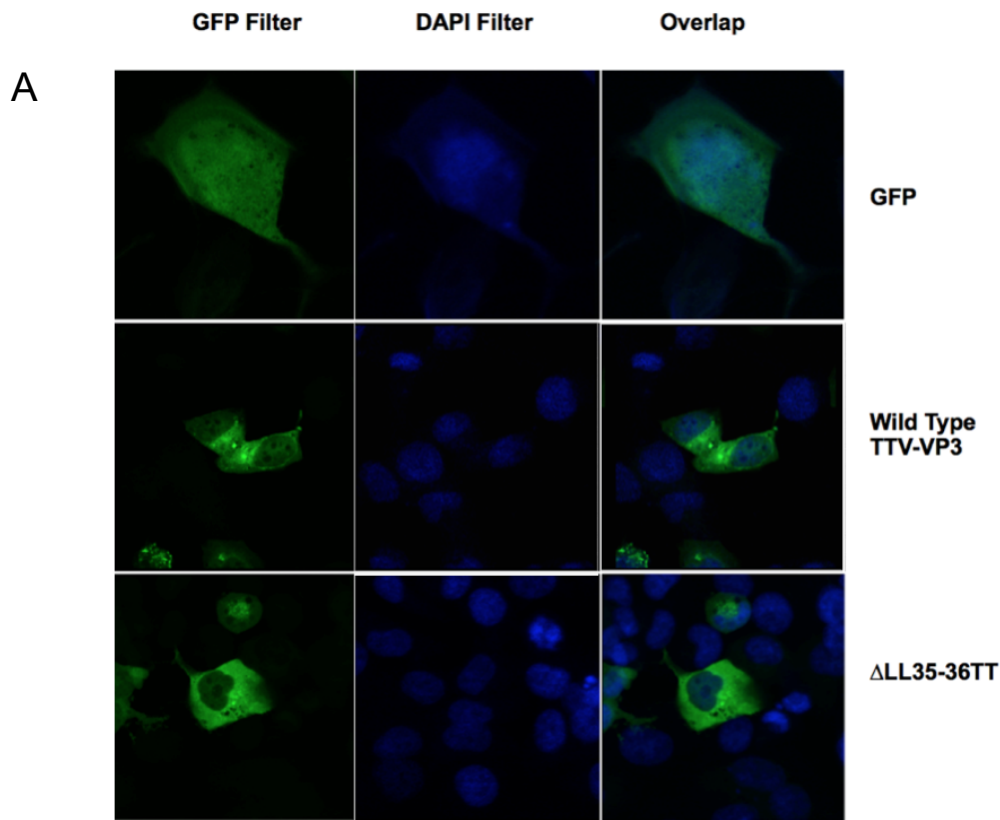


Fig. 3. Electropherograms comparing the sequences of both the wild-type and mutated TTV-VP3 constructs. The top electropherogram shows the sequence of the two leucine residues on wild-type TTV-VP3. The bottom electropherogram confirms the presence of the threonine residues in the TTV-VP3 $\Delta\Delta LL35-36TT$ construct after Quickchange PCR.



B

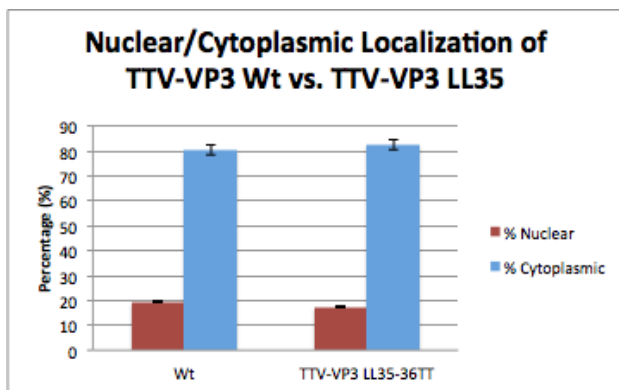


Fig. 4A. Laser confocal microscopy images of transfected H1299 non-small lung carcinoma cells. Cells were transfected in 6-well plates and then fixed and mounted on glass slides the following day. Confocal images of the such prepared slides are shown above. The first row shows a cell transfected with GFP, the second shows cells transfected with Wild-Type TTV-VP3, and the third row row shows cells transfected with the TTV-VP3 $\Delta\Delta$ LL35-36TT construct. Each column shows the localization signals of each construct under a GFP filter, DAPI filter, and overlapping filters, respectively. GFP is dispersed evenly throughout the cell. TTV-VP3 wild-type and TTV-VP3 $\Delta\Delta$ LL35-36TT show similar steady-state localization favoring the cytoplasm. **Fig. 4B.** Nuclear to cytoplasmic localization comparing the TTV-VP3 Wt and TTV-VP3 $\Delta\Delta$ LL35-36TT constructs normalized against GFP localization. Data was quantified using ImageJ software. The difference between TTV-VP3 Wt and TTV-VP3 $\Delta\Delta$ LL35-36TT nuclear-to-cytoplasmic ratio is insignificant since the error bars overlap each other. This means that the localization of TTV-VP3 was not affected by the mutation.

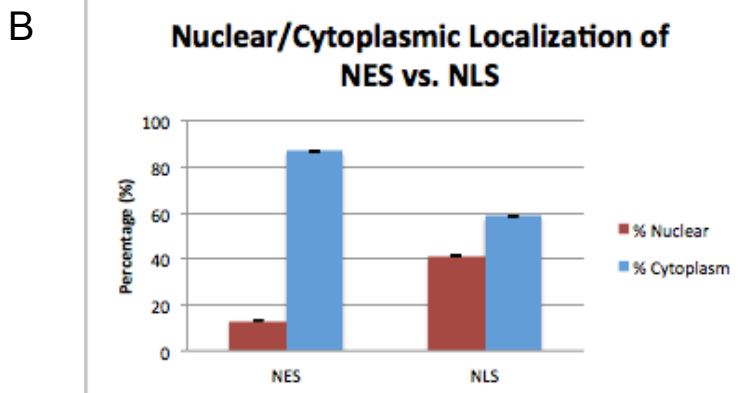
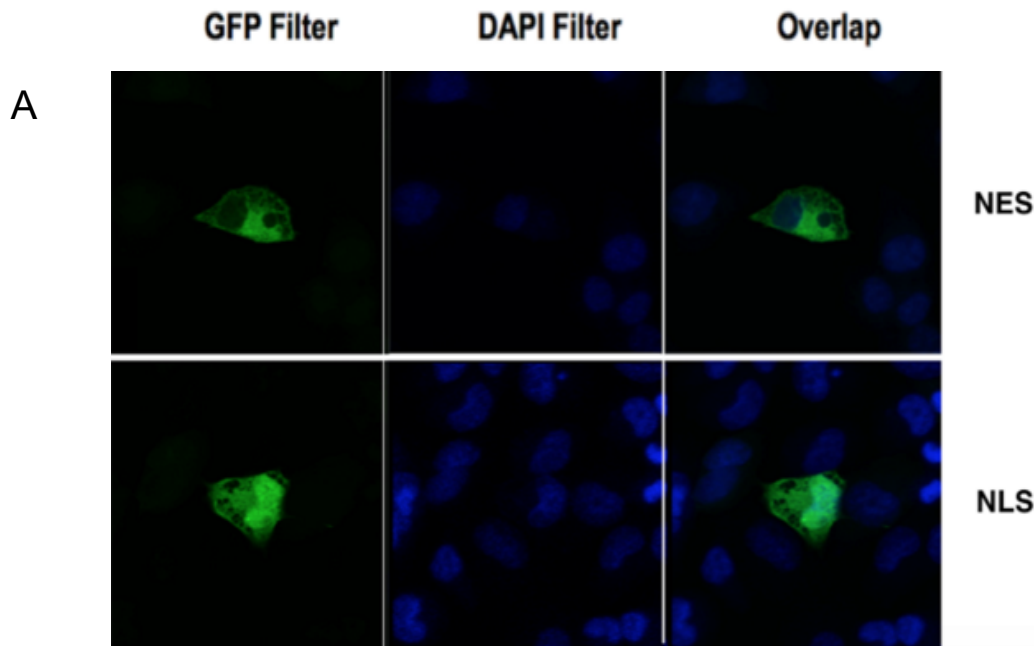


Fig. 5A. Laser confocal microscopy images of transfected H1299 non-small lung carcinoma cells. Cells were transfected in 6-well plates and then fixed and mounted on glass slides the following day. Confocal images of the prepared slides are shown above. Amino acids 1-78 of Wild-Type TTV-VP3 contain the putative nuclear export sequence (NES) and amino acids 79-105 contain the putative nuclear localization sequence (NLS). The cells shown were each transfected with these specific DNA truncations. Each column shows the localization signals of the constructs under a GFP filter, DAPI filter, and overlapping filters, respectively. The NES is largely localized in the nucleus. The NLS shows steady-state localization favoring the nucleus. **Fig. 5B.** Nuclear-to-cytoplasmic localization comparing the NES and NLS constructs normalized against GFP localization. Data was quantified using ImageJ software. The difference between NES and NLS nuclear-to-cytoplasmic ratio shows that NES favors the cytoplasm while NLS is present in the nucleus in higher amounts.

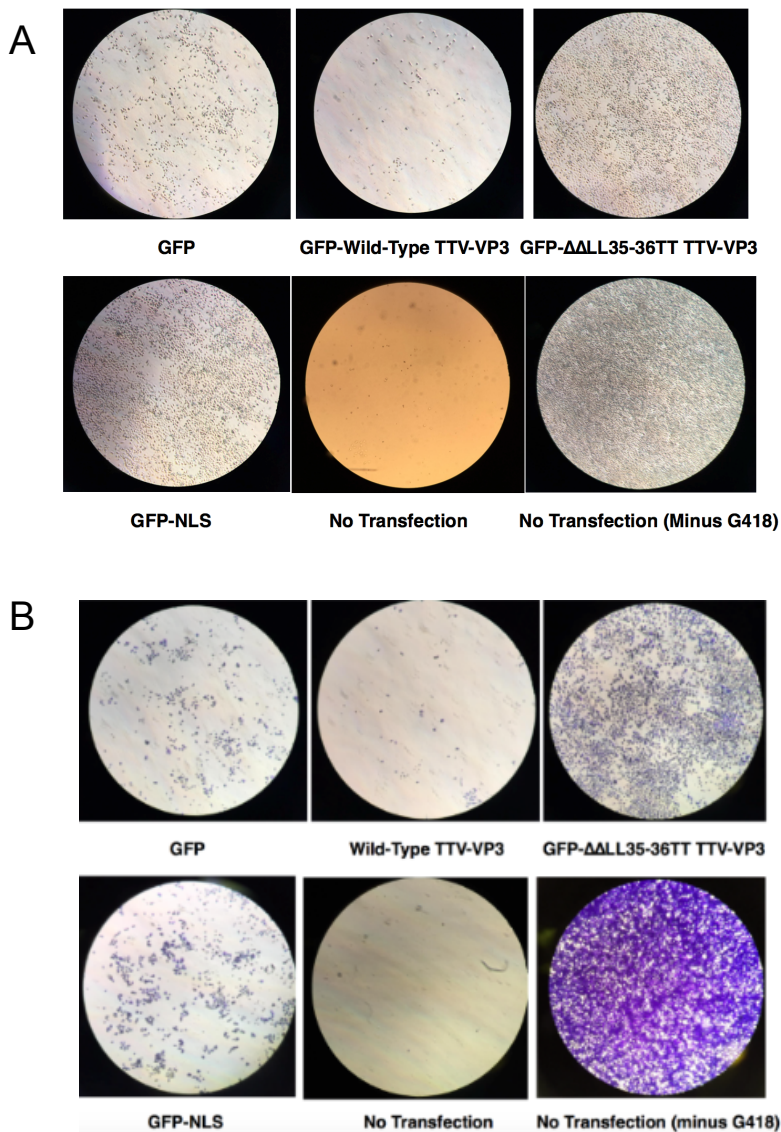


Fig. 6A. Viability assay of H1299 non-small lung carcinoma cells before crystal violet staining. **Fig. 6B.** Crystal Violet stain under 50X magnification. Aside from the “No Transfection (minus G418)” well, each well was treated with G418 to kill all transfection-negative cells. Remaining live cells were fixed to the plate with cold ethanol and stained with crystal violet. The confluence of stained cells is inversely proportional to the killing capacity of the construct transfected into the well. After all construct-negative cells were eliminated by G418, construct-positive cells were killed if the construct was able to induce apoptosis. The “GFP” well is a control. It contains transfection-positive cells that remain viable because the GFP construct is non-lethal. If other transfection-positive wells have equal amounts or more viable cells than the “GFP” well, then the construct is non-lethal. The well containing Wild-Type TTV-VP3 has less viable cells than the GFP control and therefore has killing ability. Contrarily, the $\Delta\Delta\text{LL35-36TT}$ and NLS constructs have more viable cells in their wells than the GFP control and therefore do not induce apoptosis. The “No Transfection (minus G418)” well was not treated with the G418 drug and, as expected, produces a lawn of cells.

References

1. Hino S, Miyata H. Torque teno virus (TTV): current status. *Reviews in Medical Virology*. 2007 January;17(1):45-57.
2. Nishizawa T, Okamoto H, Konishi K, Yoshizawa H, Miyakawa Y, Mayumi M. A Novel DNA Virus (TTV) Associated with Elevated Transaminase Levels in Posttransfusion Hepatitis of Unknown Etiology. *Biochemical and Biophysical Research Communications*. 1997;241(1):92-7.
3. Mushahwar IK, Erker JC, Muerhoff AS, Leary TP, Simons JN, Birkenmeyer LG, et al. Molecular and Biophysical Characterization of TT Virus: Evidence for a New Virus Family Infecting Humans. *Proceedings of the National Academy of Sciences of the United States of America*. 1999 March 16;96(6):3177-82.
4. Los M, Panigrahi S, Rashedi I, Mandal S, Stetefeld J, Essmann F, et al. Apoptin, a tumor-selective killer. *Biochimica et biophysica acta*. 2009 August;1793(8):1335.
5. Destin W, Heilman, Jose G, Teodoro, Michael R, Green. Apoptin Nucleocytoplasmic Shuttling Is Required for Cell Type-Specific Localization, Apoptosis, and Recruitment of the Anaphase-Promoting Complex/Cyclosome to PML Bodies. *Journal of Virology*. 2006 August 1;80(15):7535-45.
6. Teodoro JG, Heilman DW, Parker AE, Green MR. The viral protein Apoptin associates with the anaphase-promoting complex to induce G2/M arrest and apoptosis in the absence of p53. *Genes & development*. 2004 August 15;18(16):1952-7.
7. DeConti D, Medeiros A. Uncoupling the Multimerization and Nuclear Export Activities of CAV VP3 via Site-Directed Mutagenesis [dissertation]. Worcester Polytechnic Institute; 2008.
8. Hironori Miyata, Hiroaki Tsunoda, Aslamuzzaman Kazi, Akio Yamada, Mohammed Ali Khan, Jun Murakami, et al. Identification of a Novel GC-Rich 113-Nucleotide Region To Complete the Circular, Single-Stranded DNA Genome of TT Virus, the First Human Circovirus. *Journal of Virology*. 1999 May 1;73(5):3582-6.
9. Eric Evan-Browning, McGhee Orme-Johnson. Gene synthesis and expression of human torque teno virus VP3: Exploring the cancer-killing potential of an apoptin homologue [dissertation]. Worcester Polytechnic Institute; 2009.

10. McCauley S, Stone NP. Determining Localization Domains and Apoptotic Ability of the Human Torque Teno Virus VP3 Protein [dissertation]. Worcester Polytechnic Institute; 2011.
11. McCauley, S. Stone, N. P. Determining Localization Domains and Apoptotic Ability of the Human Torque Teno Virus VP3 Protein.
12. Nguyen KT, Holloway MP, Altura RA. The CRM1 nuclear export protein in normal development and disease. *International journal of biochemistry and molecular biology*. 2012;3(2):137-51.
13. Nguyen KT, Holloway MP, Altura RA. The CRM1 nuclear export protein in normal development and disease. *International journal of biochemistry and molecular biology*. 2012;3(2):137-51.
14. la Cour T, Kierner L, Mølgaard A, Gupta R, Skriver K, Brunak S. Analysis and prediction of leucine-rich nuclear export signals. *Protein engineering, design & selection : PEDS*. 2004 June;17(6):527-36.
15. Filatava EJ, Vu PT. Truncation mutagenesis of Porcine Circovirus 1 VP3 uncovers the importance of the C-terminal extended region in inducing apoptosis in human cancer cells [dissertation]. Worcester Polytechnic Institute; 2015.